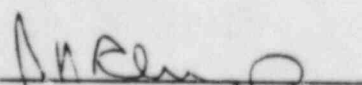


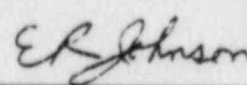
TECHNICAL BASES FOR ELIMINATING LARGE PRIMARY
LOOP PIPE RUPTURE AS THE STRUCTURAL DESIGN
BASIS FOR PRAIRIE ISLAND UNIT 1

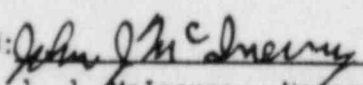
September, 1984

S. A. Swamy
Y. S. Lee

R. A. Holmes
H. F. Clark, Jr.

APPROVED: 
J. N. Chirigos, Manager
Structural Materials Engineering

APPROVED: 
E. R. Johnson, Manager
Structural and Seismic
Development

APPROVED: 
J. J. McInerney, Manager
Mechanical Equipment and
Systems Licensing

WESTINGHOUSE ELECTRIC CORPORATION
Nuclear Energy Systems
P.O. Box 355
Pittsburgh, Pennsylvania 15200

FOREWORD

This document contains Westinghouse Electric Corporation proprietary information and data which has been identified by brackets. Coding associated with the brackets set forth the basis on which the information is considered proprietary. These codes are listed with their meanings in WCAP-7211.

The proprietary information and data contained in this report were obtained at considerable Westinghouse expense and its release could seriously affect our competitive position. This information is to be withheld from public disclosure in accordance with the Rules of Practice, 10 CFR 2.790 and the information presented herein be safeguarded in accordance with 10 CFR 2.903. Withholding of this information does not adversely affect the public interest.

This information has been provided for your internal use only and should not be released to persons or organizations outside the Directorate of Regulation and the ACRS without the express written approval of Westinghouse Electric Corporation. Should it become necessary to release this information to such persons as part of the review procedure, please contact Westinghouse Electric Corporation, which will make the necessary arrangements required to protect the Corporation's proprietary interests.

The proprietary information is deleted in the unclassified version of this report.

TABLE OF CONTENTS

<u>Section</u>	<u>Title</u>	<u>Page</u>
1.0	INTRODUCTION	1-1
1.1	Purpose	1-1
1.2	Scope	1-1
1.3	Objectives	1-1
1.4	Background Information	1-2
2.0	OPERATION AND STABILITY OF THE PRIMARY SYSTEM	2-1
2.1	Stress Corrosion Cracking	2-1
2.2	Water Hammer	2-2
2.3	Low Cycle and High Cycle Fatigue	2-3
3.0	PIPE GEOMETRY AND LOADING	3-1
4.0	FRACTURE MECHANICS EVALUATION	4-1
4.1	Global Failure Mechanism	4-1
4.2	Local Failure Mechanism	4-2
4.3	Material Properties	4-3
4.4	Results of Crack Stability Evaluation	4-5
5.0	LEAK RATE PREDICTIONS	5-1
5.1	Introduction	5-1
5.2	General Considerations	5-1
5.3	Calculation Method	5-1
5.4	Leak Rate Calculations	5-2
6.0	FATIGUE CRACK GROWTH ANALYSIS	6-1
7.0	ASSESSMENT OF MARGINS	7-1
8.0	CONCLUSIONS	8-1
9.0	REFERENCES	9-1
APPENDIX A-	[a,c,e]	A-1

LIST OF TABLES

<u>Table</u>	<u>Title</u>	<u>Page</u>
3-1	Prairie Island Primary Loop Data	3-3
6-1	Fatigue Crack Growth at [] ^{a,c,e}	6-3

LIST OF FIGURES

<u>Figure</u>	<u>Title</u>	<u>Page</u>
3-1	Reactor Coolant Pipe	3-4
3-2	Schematic Diagram of Primary Loop Showing Weld Locations - Prairie Island Unit 1	3-5
4-1	[σ] ^{a,c,e} Stress Distribution	4-7
4-2	J vs Δa for SA376 TP316 Wrought Stainless Steel at 600°F	4-8
4-3	J vs Δa for SA351 CF8M Cast Stainless Steel at 600°F	4-9
4-4	J- Δa Curves at Different Temperatures, Aged Material [σ] ^{a,c,e} (7500 Hours at 400°C)	4-10
4-5	"Critical" Flaw Size Prediction	4-11
5-1	Analytical Predictions of Critical Flow Rates of Steam-Water Mixtures	5-4
5-2	[σ] ^{a,c,e} Pressure Ratio as a Function of L/D	5-5
5-3	Idealized Pressure Drop Profile Through a Postulated Crack	5-6
6-1	Typical Cross-Section of [σ] ^{a,c,e}	6-4
6-2	Reference Fatigue Crack Growth Curves for [σ] ^{a,c,e}	6-5
6-3	Reference Fatigue Crack Growth Law for [σ] ^{a,c,e} in a Water Environment at 600°F	6-6
A-1	Pipe with a Through-Wall Crack in Bending	A-2

1.0 INTRODUCTION

1.1 Purpose

This report applies to the Prairie Island Unit 1 Reactor Coolant System (RCS) primary loop piping. It is intended to demonstrate that for the specific parameters of the Prairie Island plant, RCS primary loop pipe breaks need not be considered in the structural design basis. The approach taken has been accepted by the Nuclear Regulatory Commission (NRC) (Reference 1).

1.2 Scope

The structural design basis for the RCS primary loop requires that pipe breaks be postulated. In addition, protective measures for the dynamic effects associated with RCS primary loop pipe breaks have been incorporated in the Prairie Island Unit 1 plant design. However, Westinghouse has demonstrated on a generic basis that RCS primary loop pipe breaks are highly unlikely and should not be included in the structural design basis of Westinghouse plants (see Reference 2). In order to demonstrate this applicability of the generic evaluations to the Prairie Island plant, Westinghouse has performed a fracture mechanics evaluation, a determination of leak rates from a through-wall crack, a fatigue crack growth evaluation, and an assessment of margins.

1.3 Objectives

In order to validate the elimination of RCS primary loop pipe breaks for the Prairie Island plant, the following objectives must be achieved:

- a. Demonstrate that margin exists between the critical crack size and a postulated crack which yields a detectable leak rate.
- b. Demonstrate that there is sufficient margin between the leakage through a postulated crack and the leak detection capability of the Prairie Island plant.

c. Demonstrate that fatigue crack growth is negligible.

1.4 Background Information

Westinghouse has performed considerable testing and analysis to demonstrate that RCS primary loop pipe breaks can be eliminated from the structural design basis of all Westinghouse plants. The concept of eliminating pipe breaks in the RCS primary loop was first presented to the NRC in 1978 in WCAP-9283 (Reference 3). That Topical Report employed a deterministic fracture mechanics evaluation and a probabilistic analysis to support the elimination of RCS primary loop pipe breaks. That approach was then used as a means of addressing Generic Issue A-2 and Asymmetric LOCA Loads.

Westinghouse performed additional testing and analysis to justify the elimination of RCS primary loop pipe breaks. This material was provided to the NRC along with Letter Report NS-EPR-2519 (Reference 4).

The NRC funded research through Lawrence Livermore National Laboratory (LLNL) to address this same issue using a probabilistic approach. As part of the LLNL research effort, Westinghouse performed extensive evaluations of specific plant loads, material properties, transients, and system geometries to demonstrate that the analysis and testing previously performed by Westinghouse and the research performed by LLNL applied to all Westinghouse plants including Prairie Island (References 5 and 6). The results from the LLNL study were released at a March 28, 1983 ACRS Subcommittee meeting. These studies which are applicable to all Westinghouse plants east of the Rocky Mountains determined the mean probability of a direct LOCA (RCS primary loop pipe break) to be 10^{-10} per reactor year and the mean probability of an indirect LOCA to be 10^{-7} per reactor year. Thus, the results previously obtained by Westinghouse (Reference 3) were confirmed by an independent NRC research study.

Based on the studies by Westinghouse, LLNL, the ACRS, and the AIF, the NRC completed a safety review of the Westinghouse reports submitted to address asymmetric blowdown loads that result from a number of discrete break locations on the PWR primary systems. The NRC Staff evaluation (Reference 1)

concludes that an acceptable technical basis has been provided so that asymmetric blowdown loads need not be considered for those plants that can demonstrate the applicability of the modeling and conclusions contained in the Westinghouse response or can provide an equivalent fracture mechanics demonstration of the primary coolant loop integrity.

This report provides a fracture mechanics demonstration of primary loop integrity for the Prairie Island plant consistent with the NRC position for not considering asymmetric blowdown.

2.0 OPERATION AND STABILITY OF THE REACTOR COOLANT SYSTEM

The Westinghouse reactor coolant system primary loop has an operating history which demonstrates the inherent stability characteristics of the design. This includes a low susceptibility to cracking failure from the effects of corrosion (e.g., intergranular stress corrosion cracking), water hammer, or fatigue (low and high cycle). This operating history totals over 400 reactor-years, including five plants each having 15 years of operation and 15 other plants each with over 10 years of operation.

2.1 Stress Corrosion Cracking

For the Westinghouse plants, there is no history of cracking failure in the reactor coolant system loop piping. For stress corrosion cracking (SCC) to occur in piping, the following three conditions must exist simultaneously: high tensile stresses, a susceptible material, and a corrosive environment (Reference 7). Since some residual stresses and some degree of material susceptibility exist in any stainless steel piping, the potential for stress corrosion is minimized by proper material selection immune to SCC as well as preventing the occurrence of a corrosive environment. The material specifications consider compatibility with the system's operating environment (both internal and external) as well as other materials in the system, applicable ASME Code rules, fracture toughness, welding, fabrication, and processing.

The environments known to increase the susceptibility of austenitic stainless steel to stress corrosion are (Reference 7): oxygen, fluorides, chlorides, hydroxides, hydrogen peroxide, and reduced forms of sulfur (e.g., sulfides, sulfites, and thionates). Strict pipe cleaning standards prior to operation and careful control of water chemistry during plant operation are used to prevent the occurrence of a corrosive environment. Prior to being put into service, the piping is cleaned internally and externally. During flushes and preoperational testing, water chemistry is controlled in accordance with written specifications. External cleaning for Class 1 stainless steel piping includes patch tests to monitor and control chloride and fluoride levels. For

preoperational flushes, influent water chemistry is controlled. Requirements on chlorides, fluorides, conductivity, and pH are included in the acceptance criteria for the piping.

During plant operation, the reactor coolant water chemistry is monitored and maintained within very specific limits. Contaminant concentrations are kept below the thresholds known to be conducive to stress corrosion cracking with the major water chemistry control standards being included in the plant operating procedures as a condition for plant operation. For example, during normal power operation, oxygen concentration in the RCS is expected to be less than 0.005 ppm by controlling charging flow chemistry and maintaining hydrogen in the reactor coolant at specified concentrations. Halogen concentrations are also stringently controlled by maintaining concentrations of chlorides and fluorides within the specified limits. This is assured by controlling charging flow chemistry and specifying proper wetted surface materials.

2.2 Water Hammer

Overall, there is a low potential for water hammer in the RCS since it is designed and operated to preclude the voiding condition in normally filled lines. The reactor coolant system, including piping and primary components, is designed for normal, upset, emergency, and faulted condition transients. The design requirements are conservative relative to both the number of transients and their severity. Relief valve actuation and the associated hydraulic transients following valve opening are considered in the system design. Other valve and pump actuations are relatively slow transients with no significant effect on the system dynamic loads. To ensure dynamic system stability, reactor coolant parameters are stringently controlled. Temperature during normal operation is maintained within a narrow range by control rod position; pressure is controlled by pressurizer heaters and pressurizer spray also within a narrow range for steady-state conditions. The flow characteristics of the system remain constant during a fuel cycle because the only governing parameters, namely system resistance and the reactor coolant pump characteristics are controlled in the design process. Additionally, Westinghouse has instrumented typical reactor coolant systems to verify the flow and vibration characteristics of the system. Preoperational testing and

operating experience have verified the Westinghouse approach. The operating transients of the RCS primary piping are such that no significant water hammer can occur.

2.3 Low Cycle and High Cycle Fatigue

Low cycle fatigue considerations are accounted for in the design of the piping system through the fatigue usage factor evaluation to show compliance with the rules of Section III of the ASME Code. A further evaluation of the low cycle fatigue loadings was carried out as part of this study in the form of a fatigue crack growth analysis, as discussed in Section 6.

High cycle fatigue loads in the system would result primarily from pump vibrations. These are minimized by restrictions placed on shaft vibrations during hot functional testing and operation. During operation, an alarm signals the exceedance of the vibration limits. Field measurements have been made on a number of plants during hot functional testing, including plants similar to Prairie Island. Stresses in the elbow below the reactor coolant pump have been found to be very small, between 2 and 3 ksi at the highest. These stresses are well below the fatigue endurance limit for the material and would also result in an applied stress intensity factor below the threshold for fatigue crack growth.

3.0 PIPE GEOMETRY AND LOADING

A segment of the primary coolant hot leg pipe shown below to be limiting is sketched in Figure 3-1. This segment is postulated to contain a circumferential through-wall flaw. The inside diameter and wall thickness of the pipe are 29.2 and 2.69 inches, respectively. The pipe is subjected to a normal operating pressure of 2235 psi. Figure 3-2 identifies the loop weld locations. The material properties and the loads at these locations resulting from deadweight, thermal expansion, and Safe Shutdown Earthquake are indicated in Table 3-1. As seen from this table, the junction of the hot leg and the reactor vessel outlet nozzle is the worst location for crack stability analysis based on the highest stress due to combined pressure, dead weight, thermal expansion, and SSE (Safe Shutdown Earthquake) loading. At this location, the axial load (F_x) and the bending moment (M_b) are [

$F_x^{a,c,e}$ (including axial force due to pressure) and [$M_b^{a,c,e}$, respectively. This location will be referred to as the critical location. The loads of Table 3-1 are calculated as follows:

The axial force F and transverse bending moments, M_y and M_z , are chosen for each static load (pressure, deadweight, and thermal) based on elastic-static analyses for each of these load cases. These pipe load components are combined algebraically to define the equivalent pipe static loads F_s , M_{ys} , and M_{zs} . Based on elastic SSE response spectra analyses, amplified pipe seismic loads, F_d , M_{yd} , M_{zd} are obtained. The maximum pipe loads are obtained by combining the static and dynamic load components as follows:

$$F_x = |F_s| + |F_d|$$
$$M_b = \sqrt{M_y^2 + M_z^2}$$

where:

$$M_y = |M_{ys}| + |M_{yd}|$$
$$M_z = |M_{zs}| + |M_{zd}|$$

The normal operating loads (i.e., algebraic sum of pressure, deadweight, and 100 percent power thermal expansion loading) at the critical location, i.e., the junction of the hot leg and the reactor vessel outlet nozzle, are as follows:

$$F = [\quad]^{a,c,e} \text{ (including internal pressure)}$$

$$M = [\quad]^{a,c,e}$$

The calculated and allowable stresses for ASME III NB-3600 equation 9 (faulted i.e., pressure, deadweight, and SSE) and equation 12 (normal operating thermal stress) at the critical location are as follows:

<u>Equation Number</u>	<u>Calculated Stress (ksi)</u>	<u>Allowable Stress (ksi)</u>	<u>Ratio of Calculated/Allowable</u>
9F	[] ^{a,c,e}	50.1	[] ^{a,c,e}
12	[]	50.1	[]

TABLE 3-1

PRAIRIE ISLAND PRIMARY LOOP DATA

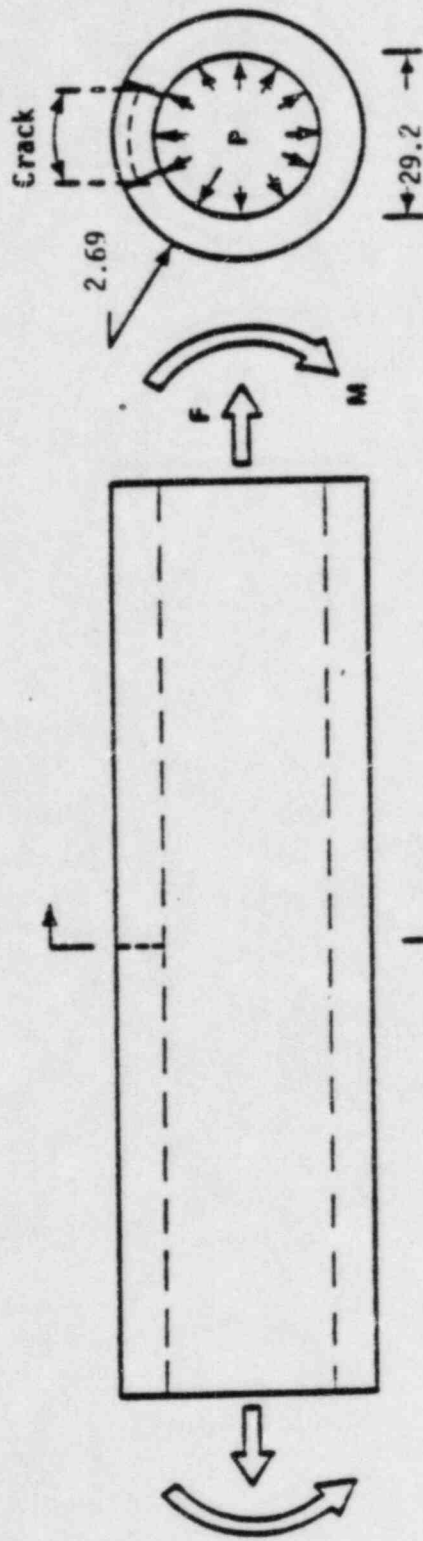
Faulted Loads^a

a,c,e

3-3

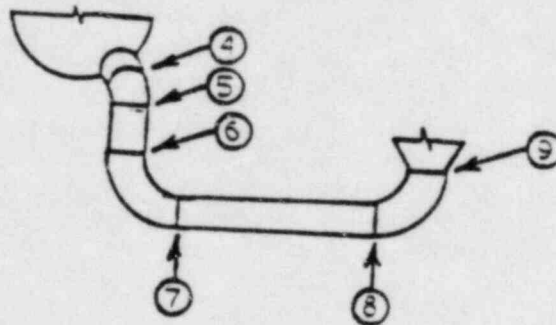
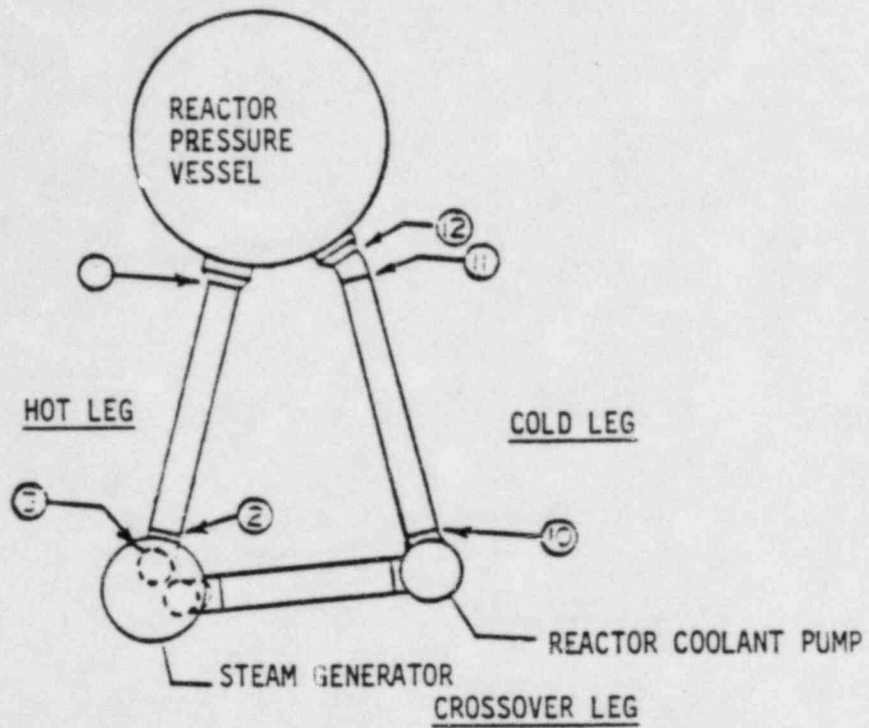
- a Includes internal pressure
- b Critical Location

Note: The piping material for Prairie Island Unit 1 is ASTM 376-TP316; for all fittings, the material is SA351-CF8M. Per the ASME Code, Section III, Division 1, the yield strengths are the same for the two materials; however, the ultimate stress for the SA351-CF8M is almost 5 ksi less. Consequently, the properties of SA351-CF8M are given in this table and will be used in the analyses set forth in this report even though there is no SA351-CF8M material at the critical location.



$P = 2,235 \text{ psi}$
 $\left[\begin{array}{l} \text{a,c,e} \end{array} \right]$

FIGURE 3-1 Reactor Coolant Pipe



HOT LEG

Temperature: 599°F; Pressure: 2235 psi

CROSSOVER LEG

Temperature: 536°F; Pressure: 2190 psi

COLD LEG

Temperature: 536°F; Pressure: 2290 psi

Figure 3-2 Schematic Diagram of Primary Loop Showing Weld Locations - Prairie Island Unit 1

4.0 FRACTURE MECHANICS EVALUATION

4.1 Global Failure Mechanism

Determination of the conditions which lead to failure in stainless steel must be done with plastic fracture methodology because of the large amount of deformation accompanying fracture. A conservative method for predicting the failure of ductile material is the [

] ^{a,c,e} This methodology has been shown to be applicable to ductile piping through a large number of experiments and will be used here to predict the critical flaw size in the primary coolant piping. The failure criterion has been obtained by requiring [

] ^{a,c,e} (Figure 4-1) when loads are applied. The detailed development is provided in Appendix A for a through-wall circumferential flaw in a pipe with internal pressure, axial force, and imposed bending moments. The [

] ^{a,c,e} for such a pipe is given by:

$$[\quad]^{a,c,e}$$

where:

$$[\quad]^{a,c,e}$$

[a,c,e]

The analytical model described above accurately accounts for the piping internal pressure as well as imposed axial force as they affect [a,c,e] Good agreement was found between the analytical predictions and the experimental results (Reference 8).

4.2 Local Failure Mechanism

The local mechanism of failure is primarily dominated by the crack tip behavior in terms of crack-tip blunting, initiation, extension and finally crack instability. Depending on the material properties and geometry of the pipe, flaw size, shape and loading, the local failure mechanisms may or may not govern the ultimate failure.

The stability will be assumed if the crack does not initiate at all. It has been accepted that the initiation toughness measured in terms of J_{IC} from a J-integral resistance curve is a material parameter defining the crack initiation. If, for a given load, the calculated J-integral value is shown to be less than the J_{IC} of the material, then the crack will not initiate. If the initiation criterion is not met, one can calculate the tearing modulus as defined by the following relation:

$$T_{app} = \frac{dJ}{da} \frac{\epsilon}{\sigma_f^2}$$

where:

T_{app} = applied tearing modulus

E = modulus of elasticity

$\sigma_f = [\quad]^{a,c,e}$ (flow stress)

a = crack length

[]^{a,c,e}

In summary, the local crack stability will be established by the two-step criteria:

$$J < J_{Ic}$$

$$T_{app} < T_{mat} \quad \text{if } J \geq J_{Ic}$$

In this analysis, a hypothesized circumferential through-wall [$\quad]^{a,c,e}$ flaw is taken as a reference flaw and is used as a basis for evaluation.

4.3 Material Properties

The primary loop piping material for Prairie Island Unit 1 is ASTM 376-TP316^a, a wrought product form. The material for the primary loop fittings is SA351-CF8M, a cast product form. Welds exist as indicated in Figure 3-2. The minimum yield stress for these materials, namely SA376-TP316 and SA351-CF8M, given in the ASME Code Section III, Division 1 are the same. The ultimate stress for the cast product form is somewhat less and is used in this report.

The tensile and flow properties of the critical location, the hot leg and the reactor vessel nozzle junction, are given in Table 3-1.

^a The ASTM designation is the information of record and predates the SA designation.

The pre-service fracture toughness of both the wrought and cast materials in terms of J have been found to be very high at 600°F. Typical results are given in Figures 4-2 and 4-3 taken from References 9. J_{IC} is observed to be well over 2000 in-lbs/in². However, cast stainless steels are subject to thermal aging during service. This thermal aging causes an elevation in the yield strength of the material and a degradation of the fracture toughness, the degree of degradation being proportional to the level of ferrite in the material. To determine the effects of thermal aging on piping integrity, a detailed study was carried out in Reference 10. In this report, fracture toughness results were presented for a material representative of []^{a,c,e}. Toughness results were provided for the material in the fully aged condition and these properties are also presented in Figure 4-4 of this report for information. The J_{IC} value for this material at operating temperature was approximately []^{a,c,e} and the maximum value of J obtained in the tests was in excess of []^{a,c,e}. The tests of this material were conducted on small specimens and therefore rather short crack extensions, (maximum extension 4.3 mm) so it is expected that higher J values would be sustained for larger specimens. []

] ^{a,c,e}

Therefore, per Ref. 10 it may be concluded that the degree of thermal aging expected by end-of-life is less than that which was produced in []^{a,c,e}. Hence, the J_{IC} values for Prairie Island Unit 1 at end-of-life would be expected to be considerably higher than those reported for []^{a,c,e} in Figure 4-4 (also see Reference 11). In addition, the tearing modulus for the Prairie Island Unit 1 materials would be greater than []^{a,c,e}.

Available data on aged stainless steel welds (Reference 10 and 11) indicate the J_{IC} values for the worst case welds are of the same order as the aged material, but the slope of the J-R curve is steeper, and higher J-values have been obtained from fracture tests (in excess of 3000 in-lbs/in²). The

applied value of the J-integral for a flaw in the weld regions will be lower than that in the base metal because the yield stress for the weld materials is much higher at temperature. Therefore, weld regions are less limiting than the cast material.

In the fracture mechanics analyses that follow, the fracture toughness properties of []^{a,c,e} discussed above will be used as the criterion against which the applied fracture toughness values will be compared.

4.4 Results of Crack Stability Evaluation

Figure 4-5 shows a plot of the []^{a,c,e} as a function of through-wall circumferential flaw length in the []^{a,c,e} of the main coolant piping. This []^{a,c,e} was calculated for Prairie Island from data for a pressurized pipe at 2235 psi with an axial force of []^{a,c,e}, operating at 599°F with []^{a,c,e} properties. The maximum applied bending moment of []^{a,c,e} in-kips can be plotted on this figure, and used to determine a critical flaw length, which is shown to be []^{a,c,e} inches.

In Table 3-1, the outer surface axial stress (σ_a) at the critical location is seen to be []^{a,c,e}. Stresses due to the internal pressure of 2235 psi are as follows (see Reference 12):

σ_c (circumferential stress): 11.1 ksi

σ_r radial stress: 0

The von Mises effective stress, σ_{eff} , (see Reference 13) is given by

$$\sigma_{eff} = \frac{1}{\sqrt{2}} \sqrt{(\sigma_a - \sigma_r)^2 + (\sigma_c - \sigma_r)^2 + (\sigma_a - \sigma_c)^2}$$

and is []^{a,c,e}.

Thus the effective stress is less than the yield stress and by the Von Mises plasticity theory yielding does not occur. Hence, linear elastic fracture mechanics is applicable for analyzing the pipe with hypothesized flaws. The analytical method used for the local stability evaluation is summarized below.

The stress intensity factors corresponding to tension and bending are expressed, respectively, by (see Reference 14)

$$K_t = \sigma_t \sqrt{\pi a} F_t(\alpha)$$

$$K_b = \sigma_b \sqrt{\pi a} F_b(\alpha)$$

where $F_t(\alpha)$ and $F_b(\alpha)$ are stress intensity calibration factors corresponding to tension and bending, respectively, α is the half-crack angle, σ_t is the remote uniform tensile stress, and σ_b is the remote fiber stress due to pure bending. Data for $F_t(\alpha)$ and $F_b(\alpha)$ are given in Reference 15. The effect of the yielding near the crack tip can be incorporated by Irwin's plastic zone correction method (see Reference 15) in which the crack length, a , in these formulas is replaced by the effective crack length, a_{eff} , defined by

$$a_{eff} = a + \frac{1}{2\pi} \frac{K^2}{\sigma_y^2}$$

for plane stress plastic corrections, where σ_y is the yield strength of the material and K is the total stress intensity due to combined tensile and bending loads. Finally, the J_I -value is determined by the relation $J_I = K^2/E$, where E = Young's Modulus (25.3×10^6 psi).

J was calculated for a through-wall flaw []^{a,c,e} inches long (the reference flaw) and found to be []^{a,c,e} in-lbs/in². The flaw was increased by 50% []^{a,c,e} and J was found to be []^{a,c,e}. Both of these values are less than J_{Ic} for the worst case []^{a,c,e} cast material described above. Thus crack initiation is not expected to occur in the Prairie Island piping even for circumferential through-wall flaws up to []^{a,c,e} inches long under the loading conditions given.

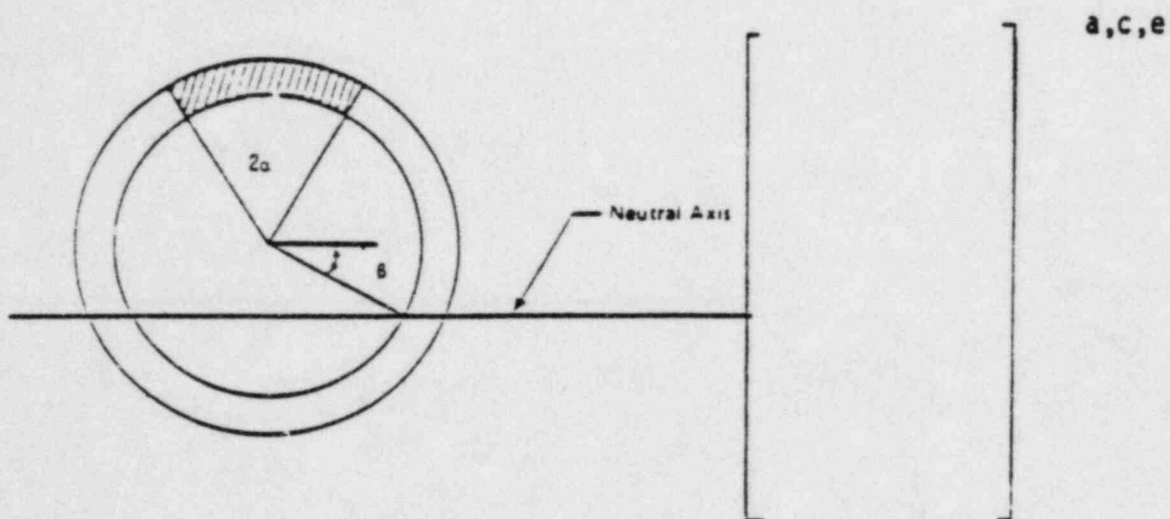


FIGURE 4-1 [a, c, e] STRESS DISTRIBUTION

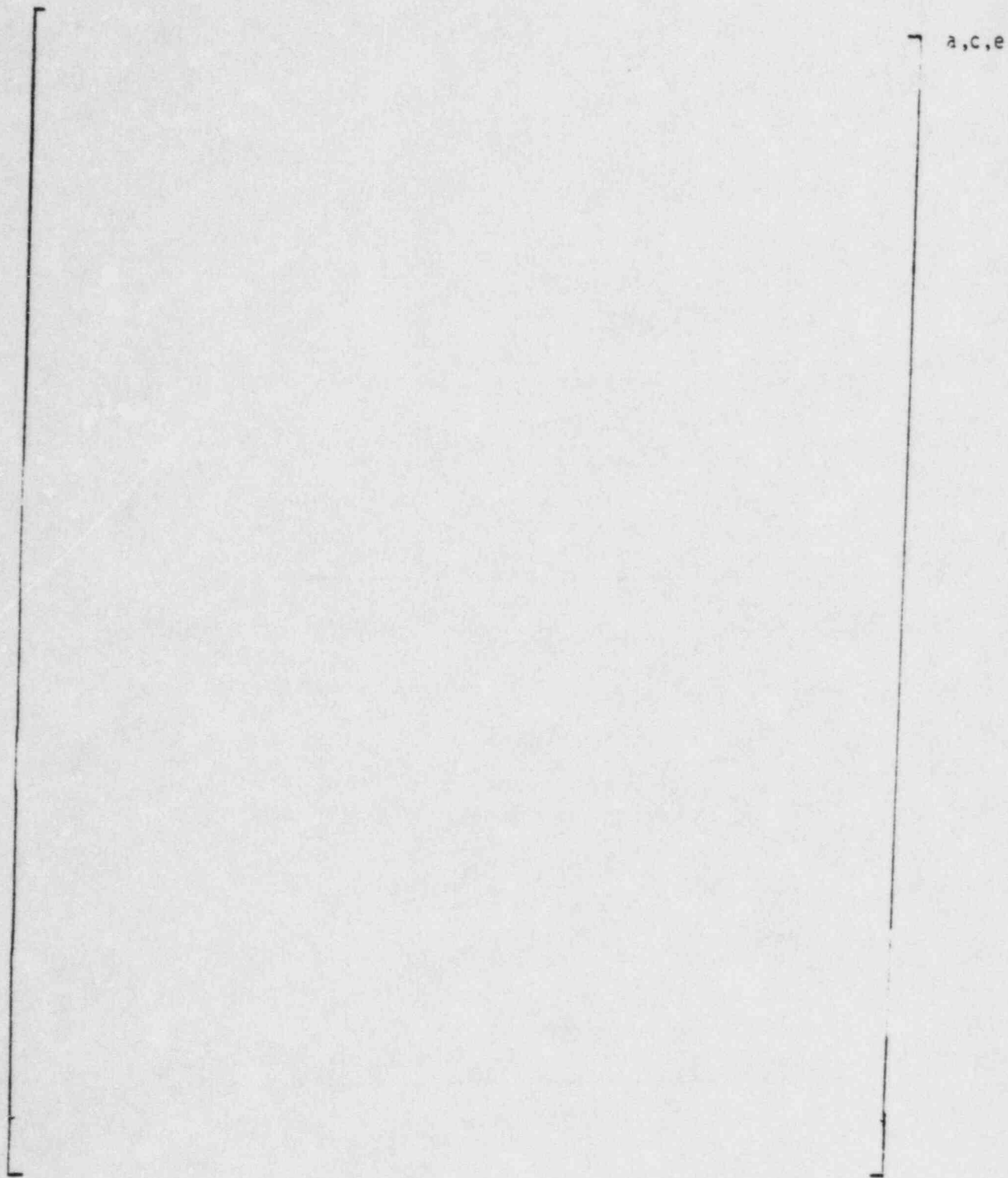


Figure 4-2 J vs Δa for SA376 TP316 Wrought Stainless Steel at 600°F

a,c,e

Figure 4-3 J vs Δa for SA351-CF8M Cast Stainless Steel at 600°F

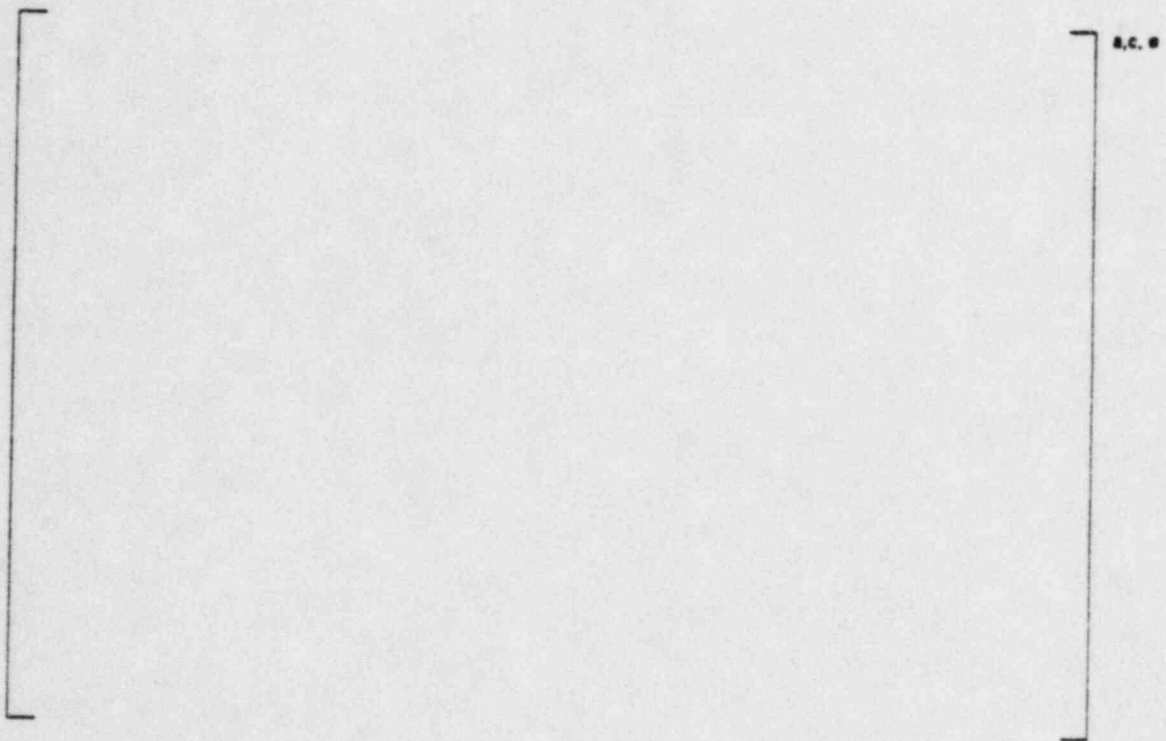
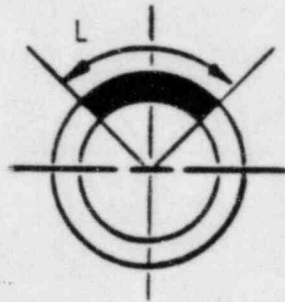


FIGURE 4-4 J- Δa Curves at Different Temperatures for Aged Material []^{a,c,e}
(7500 Hours at 400°C)

a,c,e



FLAW GEOMETRY

OD = 34.58 in.

t = 2.69 in.

p = 2235 psi

Figure 4-5 "Critical" Flaw Size Prediction

5.0 LEAK RATE PREDICTIONS

5.1 Introduction

Fracture mechanics analysis has shown that postulated through-wall cracks in the primary loop would remain stable and not cause a gross failure of this component. If such a through-wall crack did exist, it would be desirable to detect the leakage such that the plant could be brought to a safe shutdown condition. The purpose of this section is to discuss the method which will be used to predict the flow through such a postulated crack and present the leak rate calculation results for through-wall circumferential cracks.

5.2 General Considerations

The flow of hot pressurized water through an opening to a lower back pressure causes flashing which can result in choking. For long channels where the ratio of the channel length, L , to hydraulic diameter, D_H , (L/D_H) is greater than []^{a,c,e}, both []^{a,c,e} must be considered. In this situation the flow can be described as being single-phase through the channel until the local pressure equals the saturation pressure of the fluid. At this point, the flow begins to flash and choking occurs. Pressure losses due to momentum changes will dominate for []^{a,c,e}. However, for large L/D_H values, friction pressure drop will become important and must be considered along with the momentum losses due to flashing.

5.3 Calculation Method

The basic method used in the leak rate calculations is the method developed by []^{a,c,e} of the choked exit plane, as

The flow rate through a crack was calculated in the following manner. Figure 5-1 from Reference 16 was used to estimate the critical pressure, P_c , for the primary loop enthalpy condition and an assumed flow. Once P_c was found for a given mass flow, the []^{a,c,e}

was found from Figure 5-2 taken from Reference 16. For all cases considered, since []^{a,c,e} Therefore, this method will yield the two-phase pressure drop due to momentum effects as illustrated in Figure 5-3. Now using the assumed flow rate G, the frictional pressure drop can be calculated using

$$\Delta P_f = \left[\right]^{a,c,e} \quad (5-1)$$

where the friction factor f is determined using the []^{a,c,e} The crack relative roughness, c, was obtained from fatigue crack data on stainless steel samples. The relative roughness value used in these calculations was []^{a,c,e} RMS.

The frictional pressure drop using Equation 5-1 is then calculated for the assumed flow and added to the []^{a,c,e} to obtain the total pressure drop from the primary system to the atmosphere. That is, for the primary loop

$$\text{Absolute Pressure} - 14.7 = \left[\right]^{a,c,e} \quad (5-2)$$

for a given assumed flow G. If the right-hand side of Equation 5-2 does not agree with the pressure difference between the primary loop and the atmosphere, then the procedure is repeated until Equation 5-2 is satisfied to within an acceptable tolerance and this results in the flow value through the crack. This calculational procedure has been recommended by []^{a,c,e} for this type of []^{a,c,e} calculation.

5.4 Leak Rate Calculations

Leak rate estimates were performed by applying the normal operating bending moment of []^{a,c,e} in addition to the normal operating axial force of []^{a,c,e} These loads were applied to the hot leg pipe containing the postulated reference []^{a,c,e} through-wall

flaw and the crack opening area was estimated using the method of Reference 14. The leak rate was calculated using the two-phase flow formulation described above. The computed leak rate was []^{a,c,e}. In order to determine the sensitivity of leak rate to flaw size, a through-wall flaw []^{a,c,e} in length was postulated. The calculated leak rate was []^{a,c,e}.

The Prairie Island plant has an RCS pressure boundary leak detection system which is consistent with the guidelines of Regulatory Guide 1.45 for detecting leakage of 1 gpm in one hour. Thus, for the []^{a,c,e} inch flaw, a factor in excess of 80 exists between the calculated leak rate and the criteria of Regulatory Guide 1.45. Relative to the []^{a,c,e}, a factor of over 23 exists.

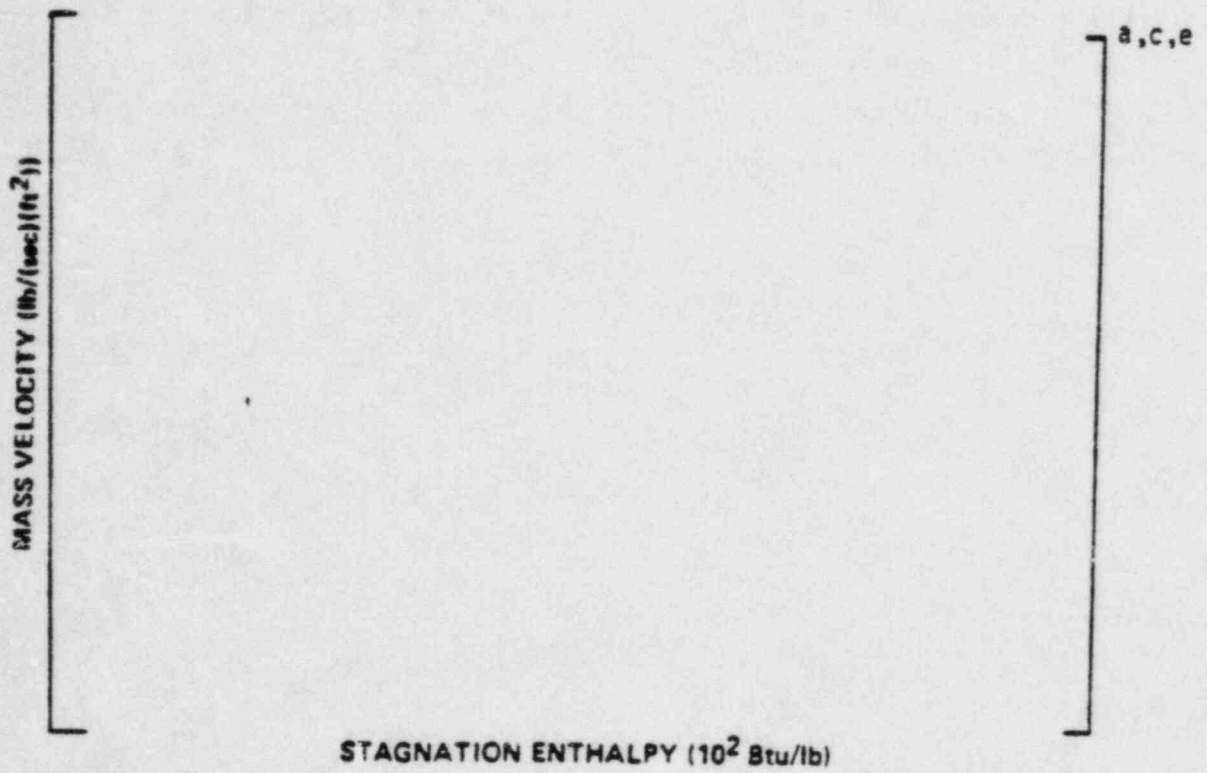


Figure 5-1 Analytical Predictions of Critical Flow Rates of Steam-Water Mixtures

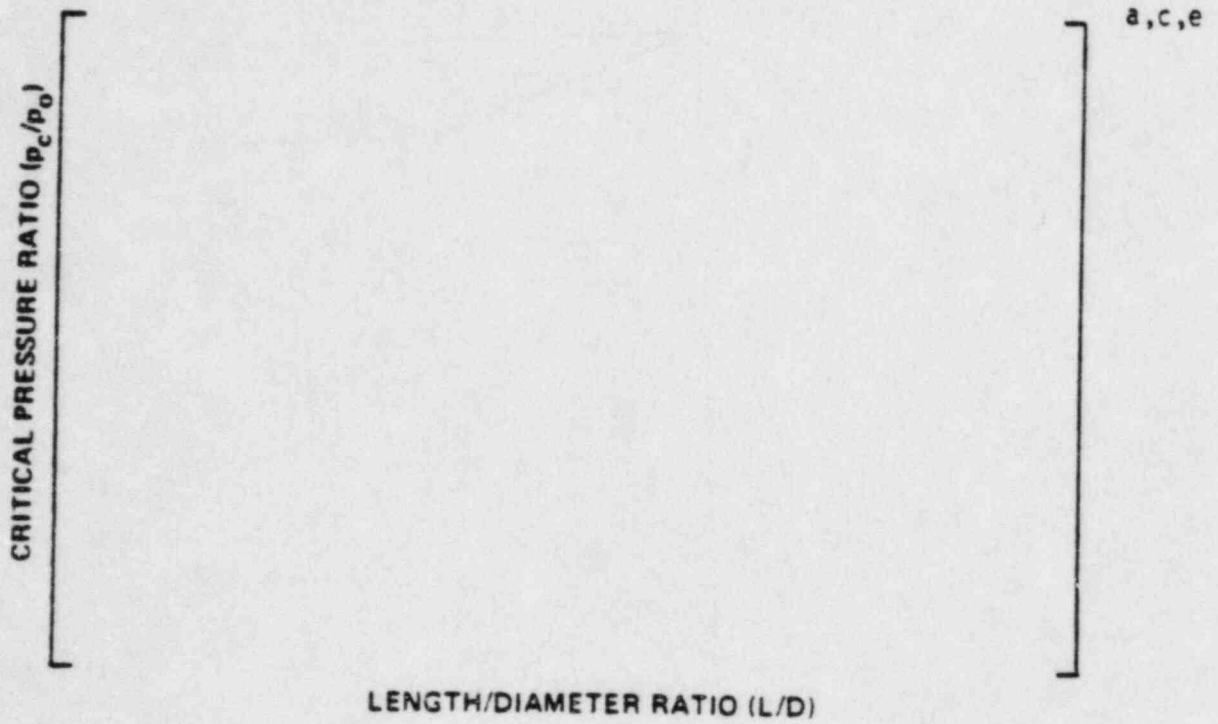


Figure 5-2 [$]^{a,c,e}$ Pressure Ratio as a Function of L/D

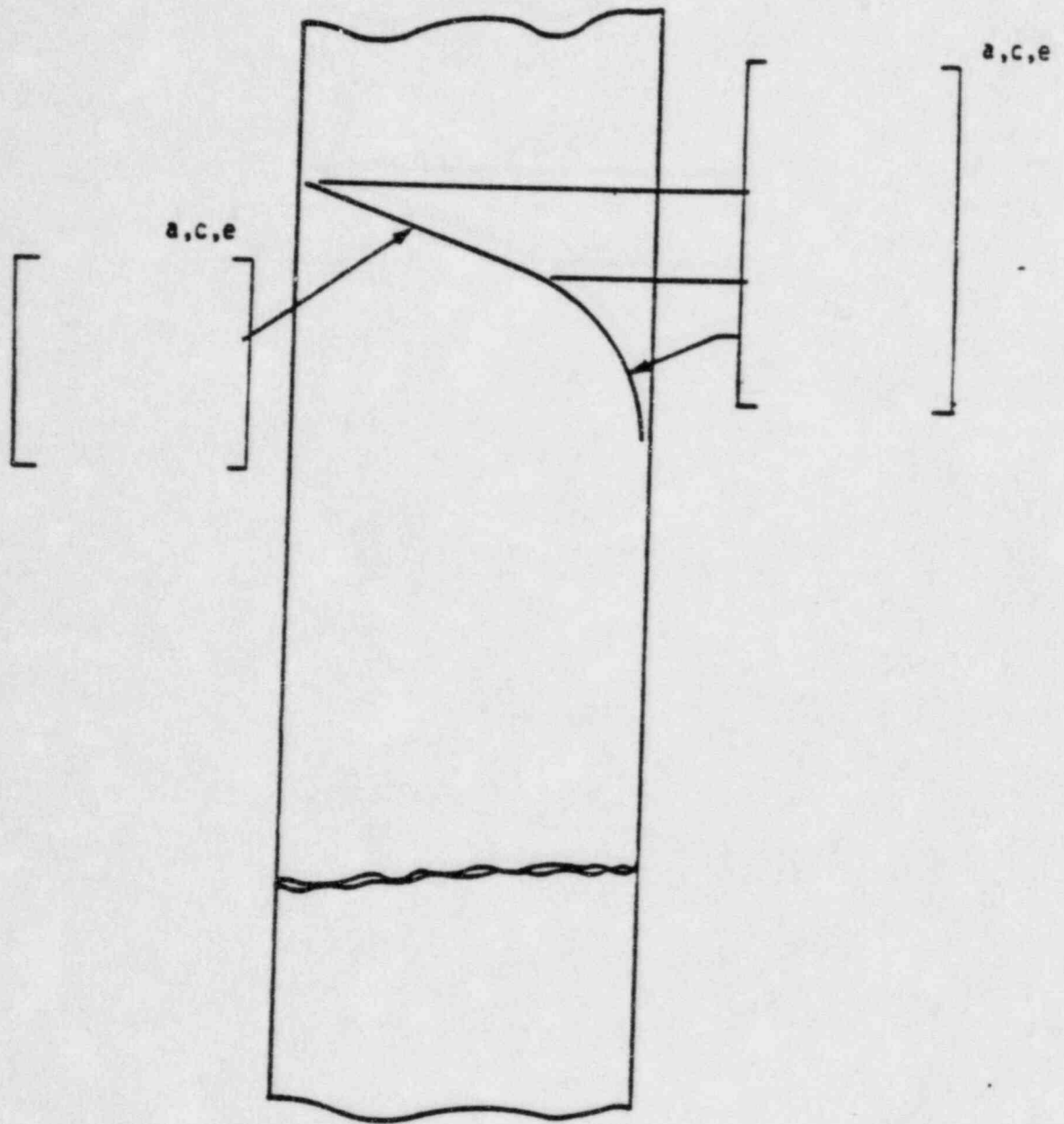


Figure 5-3 Idealized Pressure Drop Profile Through a Postulated Crack

6.0 FATIGUE CRACK GROWTH ANALYSIS

To determine the sensitivity of the primary coolant system to the presence of small cracks, a fatigue crack growth analysis was carried out for the []^{a,c,e} region of a typical system (see Location []^{a,c,e} of Figure 3-2). This region was selected because it is typically one of the highest stressed cross sections, and crack growth calculated here will be typical of that in the entire primary loop.

A []^{a,c,e} of a plant typical in geometry and operational characteristics to any Westinghouse PWR System. []

] ^{a,c,e}

All normal, upset, and test conditions were considered and circumferentially oriented surface flaws were postulated in the region, assuming the flaw was located in three different locations, as shown in Figure 6-1. Specifically, these were:

Cross Section A: []
 Cross Section B: []
 Cross Section C: [] ^{a,c,e}

Fatigue crack growth rate laws were used []

] ^{a,c,e}

The law for stainless steel was derived from Reference 18, with a very conservative correction for the R ratio, which is the ratio of minimum to maximum stress during a transient. For stainless steel, the fatigue crack growth formula is:

$$\frac{da}{dn} = (5.4 \times 10^{-12}) K_{eff}^{4.48} \text{ inches/cycle}$$

where $K_{eff} = K_{max} (1-R)^{0.5}$

$$R = K_{min} / K_{max}$$

[

] a,c,e

[

]

a,c,e

where: [

] a,c,e

The calculated fatigue crack growth for semi-elliptic surface flaws of circumferential orientation and various depths is summarized in Table 6-1, and shows that the crack growth is very small, regardless [

] a,c,e

TABLE 6-1

FATIGUE CRACK GROWTH AT []^{a,c,e} (40 YEARS)

INITIAL FLAW (IN)	FINAL FLAW (in)		
	[] ^{a,c,e}	[] ^{a,c,e}	[] ^{a,c,e}
0.292	0.31097	0.30107	0.30698
0.300	0.31949	0.30953	0.31626
0.375	0.39940	0.38948	0.40763
0.425	0.45271	0.4435	0.47421

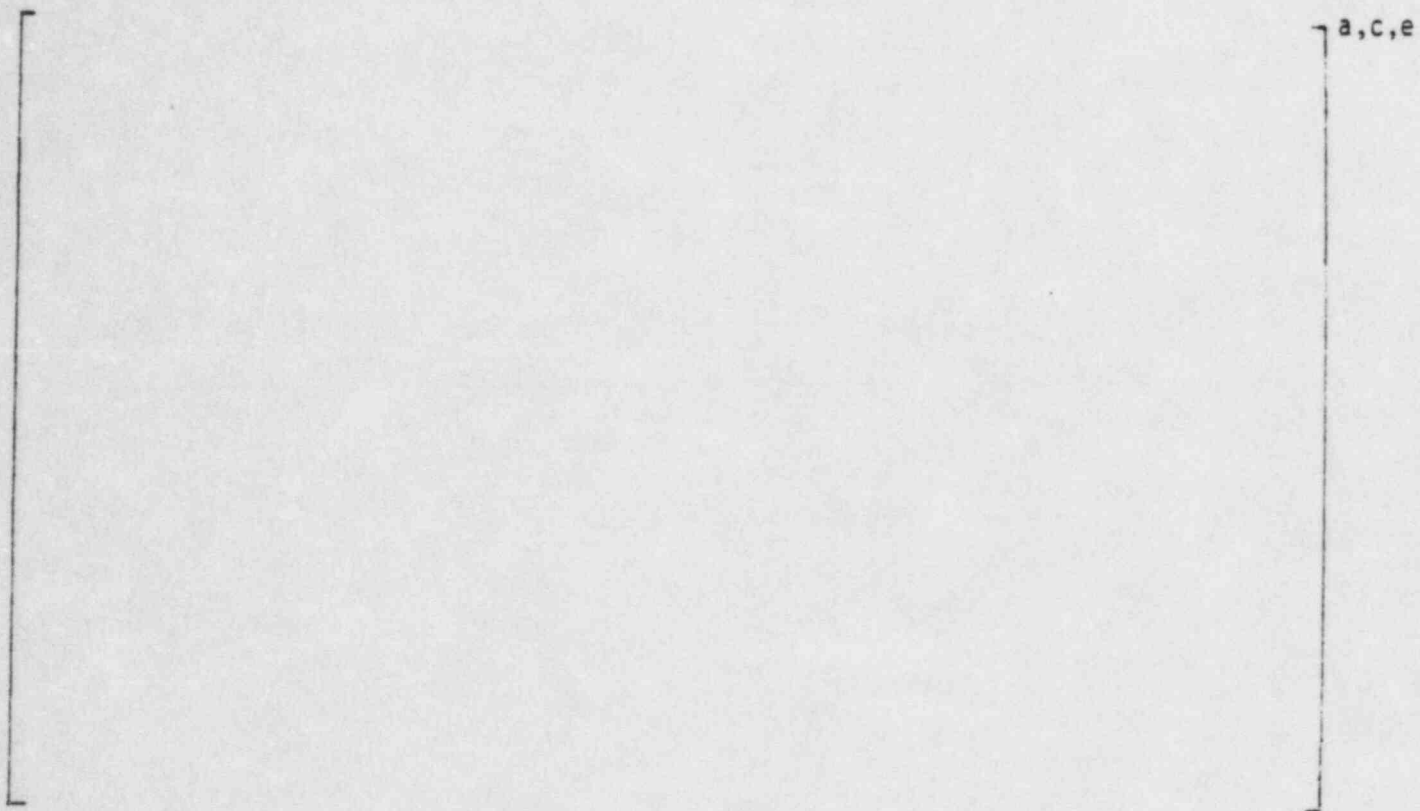
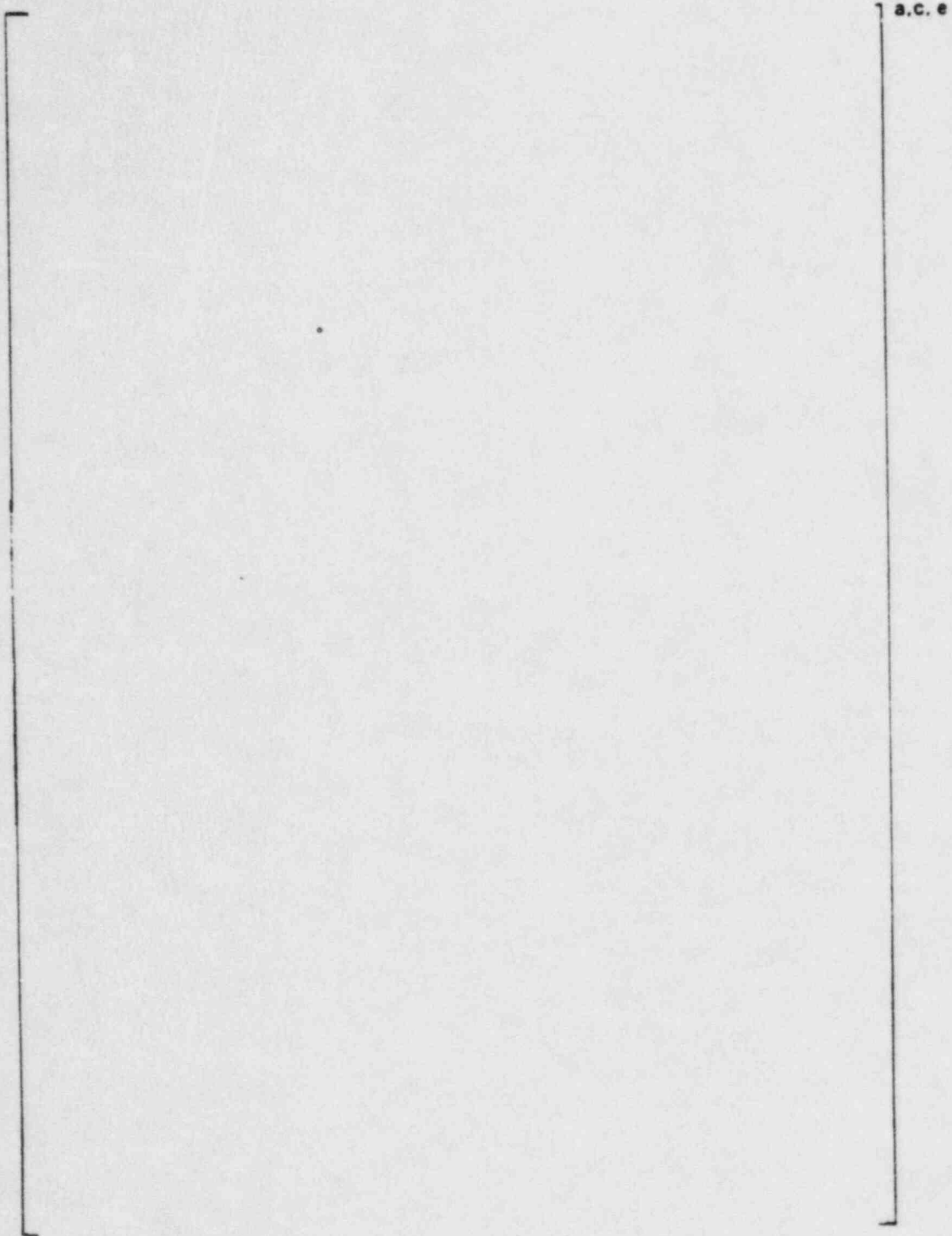


Figure 6-1 Typical Cross-Section of []^{a,c,e}

CRACK GROWTH RATE, da/dN (MICRO-INCHES/CYCLE)

a, c, e

Figure 6-2 Reference Fatigue Crack Growth Curves for [
]a, c, e



« Figure 6-3 Reference Fatigue Crack Growth Law for [in a Water Environment at 600°F

]a.c.e

7.0 ASSESSMENT OF MARGINS

For a through-wall circumferential flaw []^{a,c,e} for the faulted loading conditions. A factor of about 2 exists between this value and the critical J_{Ic} of []^{a,c,e} for fully aged cast material of chemistry worst than that existing in the Prairie Island cast fittings. Thus initiation would not be anticipated for this situation. The test results for the worst case material show J-values to near []^{a,c,e}. Increasing the hypothesized flaw by 50% to []^{a,c,e} increased the applied J to []^{a,c,e} which is still less than J_{Ic} for the fully aged material.

As shown in Section 3.0, a margin of a factor of not less than 4 exists between calculated and ASME Code allowable faulted condition and thermal stresses.

In Section 4.4, the "critical" flaw size using []^{a,c,e} method is calculated to be []^{a,c,e} inches. Based on the above, the "critical" flaw size will, of course, exceed []^{a,c,e}

In Section 5.0, it is shown that a flaw of []^{a,c,e} would yield a leak rate in excess of []^{a,c,e} while for a []^{a,c,e} inch flaw, the leak rate is over []^{a,c,e}. Thus, there is a margin of at least 4 between the flaw size that gives a leak rate well exceeding the criterion of Regulatory Guide 1.45 and the "critical" flaw size of []^{a,c,e}

In summary, relative to

1. Loads

- a. Prairie Island Unit 1 is enveloped by the J values employed in testing of fully aged material.

- b. Margins at the critical location of at least 4 on faulted conditions and thermal stresses exist relative to ASME Code allowable values.

2. Flaw Size

- a. A margin of at least 4 exists between the "critical" flaw and the flaw yielding a leak rate of []^{a,c,e}
- b. If []^{a,c,e} is used as the basis for "critical" flaw size, the margin for global stability compared to the reference flaw would be near 5.
- c. A margin of at least 50% exists between the reference flaw size []^{a,c,e} and the established minimum "critical" flaw size. Flaw initiation is shown not to occur for either case, $J < J_{Ic}$ for flaws of size of at least []^{a,c,e} inches.

3. Leak Rate

A margin in excess of 80 exists for the reference flaw []^{a,c,e} between calculated leak rates and the criteria of Regulatory Guide 1.45.

8.0 CONCLUSIONS

This report justifies the elimination of RCS primary loop pipe breaks for the Prairie Island Unit 1 plant as follows:

- a. Stress corrosion cracking is precluded by use of fracture resistant materials in the piping system and controls on reactor coolant chemistry, temperature, pressure, and flow during normal operation.
- b. Water hammer should not occur in the RCS piping because of system design, testing, and operational considerations.
- c. The effects of low and high cycle fatigue on the integrity of the primary piping are negligible.
- d. Adequate margin exists between the leak rate of the reference flaw and the criteria of Reg. Guide 1.45.
- e. Ample margin exists between the reference flaw chosen for leak detectability and the "critical" flaw.
- f. Ample margin exists in the material properties used to demonstrate end-of-life (relative to aging) stability of the reference flaw.

The reference flaw will be stable throughout reactor life because of the ample margins in d, e, and f above and will leak at a detectable rate which will assure a safe plant shutdown.

Based on the above, it is concluded that RCS primary loop pipe breaks should not be considered in the structural design basis of the Prairie Island Unit 1 plant.

9.0 REFERENCES

1. USNRC Generic letter 84-04, Subject: "Safety Evaluation of Westinghouse Topical Reports Dealing with Elimination of Postulated Pipe Breaks in PWR Primary Main Loops", February 1, 1984.
2. Letter from Westinghouse (E. P. Rahe) to NRC (R. H. Vollmer), NS-EPR-2768, dated May 11, 1983.
3. WCAP-9283, "The Integrity of Primary Piping Systems of Westinghouse Nuclear Power Plants During Postulated Seismic Events," March, 1978.
4. Letter Report NS-EPR-2519, Westinghouse (E. P. Rahe) to NRC (D. G. Eisenhut). Westinghouse Proprietary Class 2, November 10, 1981.
5. Letter from Westinghouse (E. P. Rahe) to NRC (W. V. Johnston) dated April 25, 1983.
6. Letter from Westinghouse (E. P. Rahe) to NRC (W. V. Johnston) dated July 25, 1983.
7. NUREG-0691, "Investigation and Evaluation of Cracking Incidents in Piping in Pressurized Water Reactors", USNRC, September 1980.
8. Kanninen, M. F., et. al., "Mechanical Fracture Predictions for Sensitized Stainless Steel Piping with Circumferential Cracks", EPRI NP-192, September 1976.
9. Landes, J. D., et. al., Fracture Toughness of 316 Stainless Steel Piping Material at 600°F, Westinghouse R&D Report 79-703-PIPRE-R1, May 17, 1979 (Westinghouse Proprietary Class 2).

10. WCAP-10456, "The Effects of Thermal Aging on the Structural Integrity of Cast Stainless Steel Piping For W NSSS," W Proprietary Class 2, November 1983.
11. Slama, G., Petrequin, P., Masson, S. H., and Mager, T. R., "Effect of Aging on Mechanical Properties of Austenitic Stainless Steel Casting and Welds", presented at SMIRT 7 Post Conference Seminar 6 - Assuring Structural Integrity of Steel Reactor Pressure Boundary Components, August 29/30, 1983, Monterey, CA.
12. Durelli, A. J., et. al., Introduction to the Theoretical and Experimental Analysis of Stress and Strain, McGraw Hill Book Company, New York, (1958), pp 233-236.
13. Johnson, W. and Mellor, P. B., Engineering Plasticity, Van Nostrand Reinhold Company, New York, (1973), pp 83-86.
14. Tada, H., "The Effects of Shell Corrections on Stress Intensity Factors and the Crack Opening Area of Circumferential and a Longitudinal Through-Crack in a Pipe," Section II-1, NUREG/CR-3464, September 1983.
15. Irwin, G. R., "Plastic Zone Near a Crack and Fracture Toughness," Proc. 7th Sagamore Conference, P. IV-63 (1960).
16. [

]a,c,e
17. [

]a,c,e

18. Bamford, W. H., "Fatigue Crack Growth of Stainless Steel Piping in a Pressurized Water Reactor Environment," Trans. ASME Journal of Pressure Vessel Technology, Vol. 101, Feb. 1979.

19. [

]a,c,e

20. [

]a,c,e

APPENDIX A

a,c,e



FIGURE A-1 PIPE WITH A THROUGH-WALL CRACK IN BENDING